Food Chemistry 345 (2021) 128747

Contents lists available at ScienceDirect

Food Chemistry

journal homepage: www.elsevier.com/locate/foodchem

Detecting cooking state of grilled chicken by electronic nose and computer vision techniques

Fedor S. Fedorov [a,*], Ainul Yaqin [a], Dmitry V. Krasnikov [a], Vladislav A. Kondrashov [a], George Ovchinnikov [b], Yury Kostyukevich [b], Sergey Osipenko [b], Albert G. Nasibulin [a,c,*]

[a] Laboratory of Nanomaterials, Skolkovo Institute of Science and Technology, 3 Nobel St., 121205 Moscow, Russia
[b] Center for Computational and Data-Intensive Science and Engineering, Skolkovo Institute of Science and Technology, 3 Nobel Str., 121205 Moscow, Russia
[c] Aalto University, 00076 Espoo, Finland

ARTICLE INFO

Keywords:
Chemometrics
Computer vision
Electronic nose
Food preparation
Sensory analysis

ABSTRACT

Determination of food doneness remains a challenge for automation in the cooking industry. The complex physicochemical processes that occur during cooking require a combination of several methods for their control. Herein, we utilized an electronic nose and computer vision to check the cooking state of grilled chicken. Thermogravimetry, differential mobility analysis, and mass spectrometry were employed to deepen the fundamental insights towards the grilling process. The results indicated that an electronic nose could distinguish the odor profile of the grilled chicken, whereas computer vision could identify discoloration of the chicken. The integration of these two methods yields greater selectivity towards the qualitative determination of chicken doneness. The odor profile is matched with detected water loss, and the release of aromatic and sulfur-containing compounds during cooking. This work demonstrates the practicability of the developed technique, which we compared with a sensory evaluation, for better deconvolution of food state during cooking.

1. Introduction

Control of food doneness demands the development of new protocols suitable for the growing food-cooking industry, e.g., represented by vending machines that produce freshly-cooked food; and for air cleaning systems powered by the *Internet of Things* (IoT) (Potyrailo, 2016). Moreover, in industrial kitchens, cooking in huge quantities needs an automated determination of food state to be integrated into risk or quality management. While the evaluation of food readiness is usually made by assessment of color, texture, and chemical composition changes through aroma and color perceived by the human nose and eye (Ötles, 2016), it is rather subject to the psychological and physical condition of the human.

The complexity of the aroma can be primarily evaluated using analytical techniques such as gas chromatography or mass spectrometry which are, however, rather expensive, complex, time-consuming, and require trained personnel to operate. A much simpler technique is based on gas-analytical systems made of discrete sensors that are collected in arrays for the discrimination of odors or smell patterns mimicking mammalian olfactory systems (Persaud & Dodd, 1982). Such arrays, often called electronic noses or e-noses, have been already demonstrated as a useful tool for quality control in industries concerned with odors. Recently, a number of studies have been conducted using e-nose to analyze food quality, i.e. of wine grapes (Lerma et al., 2011), coffee beans (Dong et al., 2019), pork (Huang et al., 2014), to discriminate different categories of cheeses (Schroeder et al., 2019), and to monitor fruit spoilage and maturity, for example, of apple (Li, Heinemann, & Sherry, 2007) and banana (Chen et al., 2018). E-nose was applied to monitor food production (Ponzoni et al., 2008), i.e. the key aromas of the bread baking process using an array of four metal-oxide-based sensors. Hirano et al. studied the use of e-nose to detect the cooking state of microwave popcorn and waffles (Hirano et al., 2013). However, the e-nose can only acquire the volatile compounds and ignores other attributes of food like color or appearance in general. Though the food appearance is a complex and multi-parameter value, it can be monitored with advances in computer vision. These systems are rather intensively

* Corresponding authors at: Laboratory of Nanomaterials, Skolkovo Institute of Science and Technology, 3 Nobel St., 121205 Moscow, Russia.
E-mail addresses: f.fedorov@skoltech.ru (F.S. Fedorov), ainul.yaqin@skoltech.ru (A. Yaqin), d.krasnikov@skoltech.ru (D.V. Krasnikov), v.kondrashov@skoltech.ru (V.A. Kondrashov), g.ovchinnikov@skoltech.ru (G. Ovchinnikov), y.kostyukevich@skoltech.ru (Y. Kostyukevich), sergey.osipenko@skoltech.ru (S. Osipenko), a.nasibulin@skoltech.ru (A.G. Nasibulin).

https://doi.org/10.1016/j.foodchem.2020.128747
Received 30 July 2020; Received in revised form 21 November 2020; Accepted 25 November 2020
Available online 1 December 2020

studied for integration in the technology of food processing, quality evaluation and control mainly combined with machine learning techniques (Du & Sun, 2006; Gunasekaran, 1996; Jackman & Sun, 2013). Such a high interest is because of the advantages of being fast, consistent, and objective (Brosnan & Sun, 2004), allowing many different applications like the assessment of freshness, texture, aging, or humidity of the meat surface (Taheri-Garavand et al., 2019). Although many studies are devoted to food quality, there are only a few reports on the issue of cooking and food preparation. Computer vision has been used for biscuit baking (Nashat & Abdullah, 2010; Yeh et al., 1995), beef doneness determination (Unklesbay et al., 1988), cheese melting (Wang & Sun, 2002), and for fried products (Leiva-Valenzuela et al., 2018). This method is proven objective when compared with sensorial evaluation (Greiff et al., 2015) because it relies on analytical methods of assessment of chemical processes occurring in organic tissues under heat (Farroni & del Pilar Buera, 2012; Gökmen et al., 2007).

The pattern recognition associated with both computer vision and e-nose employs various methods, statistical ones like linear discriminant analysis, and biologically motivated non-parametric methodologies, e.g. artificial neural networks (Hines et al., 2002; Jordan & Mitchell, 2015; Martinez & Kak, 2001). The employed machine learning is an exponentially growing field that has proved itself useful for complex multi-parameter tasks from image processing to chemical engineering (Iakovlev et al., 2019; Joutou & Yanai, 2009). The method has shown its best in facilitating routine data processing (Wan, Jiang, & Park, 2020) and also in the optimization of a semi-industrial process (Khabushev et al., 2019) and even catalyst design (Li, Wang, & Xin, 2018). In general, machine learning benefits multi-parametric and complex datasets that had been comprehended formerly by the human brain only. Moreover, computer vision alone cannot be fully indicative for controlling food; computer vision or machine-learning-based image analysis could be complimentary when combined with e-nose to objectively monitor the main attributes for consumer acceptability of food – odor and appearance (Di Rosa et al., 2017; Girolami et al., 2014; Keller et al., 2017). These methods also offer a contactless examination of the samples.

Chicken meat represented about 37% of global meat production in 2018 (FAO, 2018). Chicken is characterized by its pleasant odors and can be prepared using several cooking methods, which are primarily concerned with its safety, especially in the case of grilling (Hassan, Magda, & Awad, 2010; Langsrud et al., 2020). During this process, chicken is subjected to high temperature, e.g., by burning charcoal for a certain time, depending on the desired characteristics of the final product. The changes in doneness state are accompanied both by the release of distinct odors and transformations in appearance due to complex chemical modifications occurring in chicken during the grilling. Chicken flavors result from the interaction between components found in the meat such as proteins, lipids, fatty acids, and others (Hassan, Magda, & Awad, 2010). The Maillard reaction, which occurs during heating leads to the appearance of volatile compounds such as aldehydes, ketones, acids, and alcohols (Jayasena et al., 2013; Mottram, 1998; Shi & Ho, 1994). Moreover, the development of cooked chicken flavors is greatly affected by the cooking environment, namely, by temperature and time (Coggins, 2012; Da Costa & Eri, 2012). Dolara et al. reported that mutagens were not produced in meat cooked at 100 °C (Dolara, Commoner, & Vithayathil, 1979), but were produced when the meat was cooked at temperatures of 190–210 °C. Furthermore, grilling has been reported to affect the level of polycyclic aromatic hydrocarbons in chicken (Chung et al., 2011; Lee et al., 2016). Lan et al. found an increase in toxic and carcinogenic heterocyclic amine content with increasing heating time (Lan, Kao, & Chen, 2004).

Thus, the quality and safety of prepared meat primarily require new tools for control across the cooking process. Although there is an appearance of many volatile organic compounds (VOC), e-nose systems are barely applied in cooking. Moreover, computer vision and e-nose systems have not been yet combined to control food preparation processes like grilling, whilst such a technique might be very useful for automation of the cooking process and its precise control. In this study, we hypothesize that different cooking times result in different odor profiles and colors of grilled chicken, which could be detected using e-nose and computer vision techniques to evaluate and to predict the degree of readiness of the grilled chicken. Subsequently, we demonstrate the practicability of the combination of electronic nose and computer vision techniques for the cooking industry in comparison with a sensory evaluation.

2. Materials and methods

2.1. Samples preparation and processing

Fresh raw chicken breast sample without skin was purchased from a local supermarket in Moscow, Russia.

The chicken was grilled according to the following protocol. An outdoor grill was filled with approximately 1–1.5 kg of charcoal and ignited by fire. Then, chicken breast, 0.5 kg, with a thickness of about 1.5 cm, was placed on the grill pan for 40 min. To distribute the heat equally, the chicken breast was turned every 3 min during the whole grilling process. No oil or seasoning was applied to the chicken before the grilling. The temperature of the chicken sample was measured using a UT302B Infrared thermometer (Uni-Trend Technology Co., Ltd., China) just after the breast was turned over.

2.2. E-nose

To measure the changes in the environment caused by the appearance of volatile compounds, we applied a home-made e-nose which included an array of 8 commercial sensors (Hanwei Electronics), MQ-2 (smoke), MQ-3 (alcohol), MQ-4 (CH_4), MQ-5 (liquefied petroleum gas - LPG), MQ-7 (CO), MQ-8 (H_2), MQ-9 (CO, CH_4, LPG) to be denoted as CO-II, MQ-135 (NH_3, CO_2, NO_x), also temperature and humidity probes (Fig. 1e). The sensors were installed in a single metal housing to enable constant airflow supported by a ventilation fan. The e-nose was powered by means of a USB interface connected to a PC, also used for data acquisition. The signal output, sensor resistance, was measured at 1 Hz sampling rate over 140 min of total experiment time, which included signal output from the ambient air, initial charcoal burning, and grilling periods of chicken. We presented resistance transients during the grilling of chicken normalized to its resistance in the air. Sensitivity was calculated further as $\Delta R/R_{air}$, where ΔR is a change in resistance of the sensor at exposure to volatile compounds in a mixture with air and R_{air} is the resistance of the sensor at ambient air conditions taken as a reference. During the grilling process, the electronic nose was placed in the ventilation system, where the odors and smoke were pumped out.

2.3. Thermal analysis

Evaluation of the changes corresponding to the grilling process was conducted by thermogravimetric analysis (TGA) coupled with mass spectrometry (MS). To simulate the cooking process, we used rather fast heating, 50 °C/min, to 200 °C followed by a one-hour isothermal phase. The temperature of 200 °C was reached after 5–6 min from the beginning of the experiment. A sample of ca. 50 mg was filled into alumina crucible in these tests. The measurement was performed in a SiC furnace in an atmosphere of synthetic air at a flow rate of 70 sccm. The experiment was carried out with a NETZSCH STA 449 F3 Jupiter® unit coupled with 403 Aëolos Quadro quadrupole mass spectrometer (NETZSCH-Gerätebau GmbH, Selb, Germany). Selected ion monitoring (SIM) tracked 23 different mass-to-charge (m/z) ratios during the measurement. Herein we only presented SIM data from $m/z = 18, 32, 34, 44, 45, 46, 48, 64, 77, 78$ because others were not very informative to the odor profile of grilled chicken.

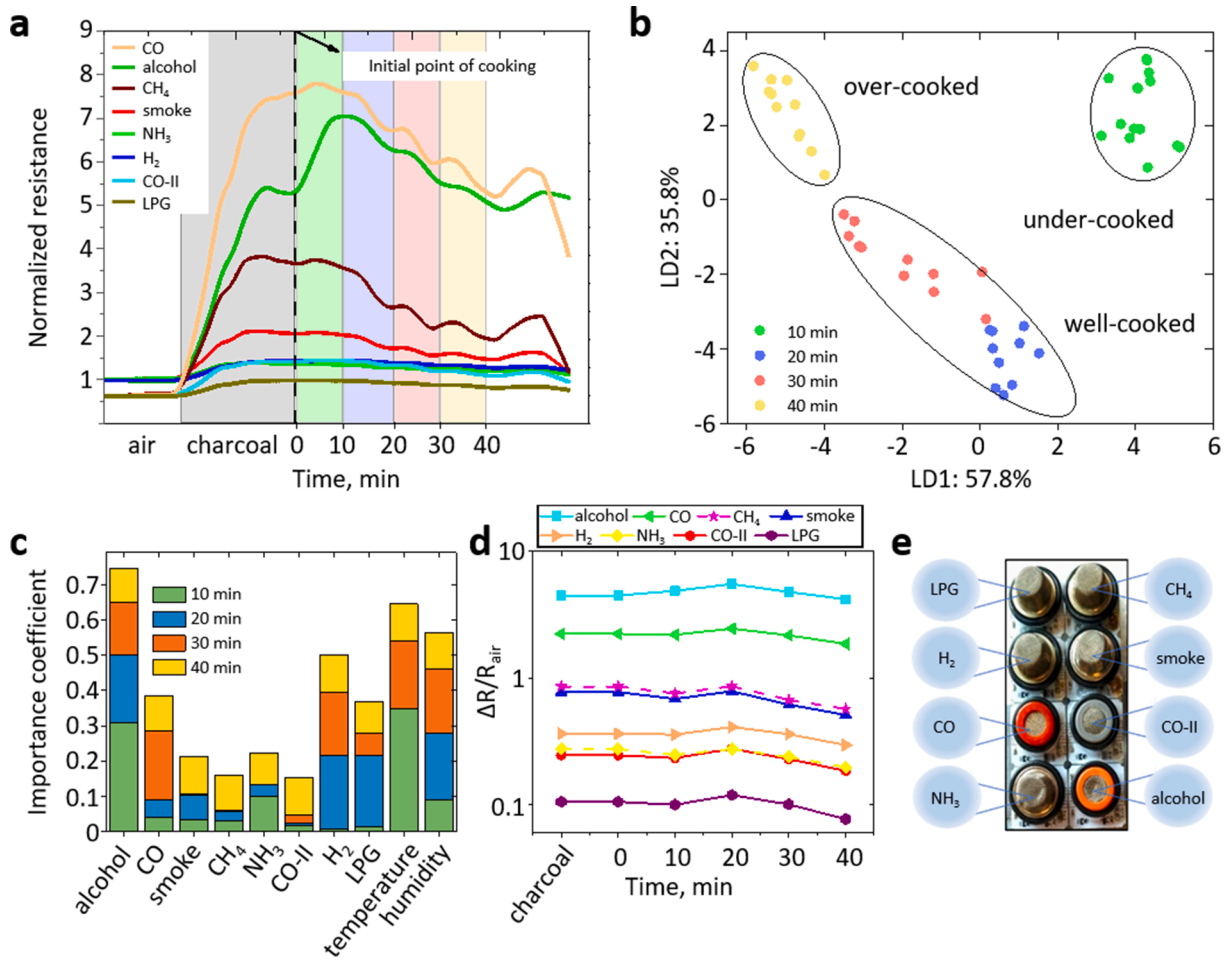

Fig. 1. Grilling state analysis based on liberated odor detection. (a) Typical transients of sensor resistance normalized to its resistance in the air during the grilling of chicken. The colors denote the difference in cooking time where the green area shows the response of 10 min, blue and red colors represent 20–30 min, and the yellow area corresponds to 40 min of cooking time. (b) Vector signals of e-nose processed by LDA and projected into a coordinate system of the first two LDA components. (c) Feature importance of the sensors in the array. (d) The sensitivity of each sensor at different cooking periods presented as $\Delta R/R_{air}$. (e) The electronic nose module overview displayed 8 sensors based on their specific interaction with target gases from alcohol to LPG. (For interpretation of the references to color in this figure legend, the reader is referred to the web version of this article.)

2.4. Differential mobility analyzer

The number size distributions of aerosol particles formed during the cooking were studied with a differential mobility analyzer (DMA) capable of measuring the particles of effective diameter from 6 nm to 230 nm (Scanning Mobility Particle Sizer Spectrometer 3938, TSI Inc., Shoreview, MN). It should be mentioned that the differential mobility analyzer measures the electrical mobility of a charged aerosol particle; then the mobility is transformed into an effective size of the measured aerosol particle with an assumption of spherical shape (standard software of Scanning Mobility Particle Sizer Spectrometer). Thus, the measured size is effective for all the dry solid particles (usually presented as clusters or non-spherical objects) and also corresponds well for liquid aerosols. For DMA studies we were able to simulate cooking conditions when a sample was usually placed already on a hot grill. Thus, during the experiment, a sample of the chicken meat (50 g) was put inside a massive muffle furnace (Nabertherm L 3/12/1340; Nabertherm GmbH, Lilienthal, Germany) at 200 °C (we consider the muffle to be isothermal during the experiment). It should be noted that the muffle itself was positioned in a zone of semi-clean air (a laminar hood) to reduce the background aerosol noise on the one hand but to preserve "natural conditions" on the other. During the experiment, the sampling was continuous with a period of 75 s.

2.5. Mass spectrometry

We applied mass spectrometry to assess further compounds of higher molecular weight which evolved during the grilling. All experiments were performed on a modified QExactive Orbitrap mass spectrometer (Thermo Scientific, Germany) with installed ion funnel and fore vacuum matrix-assisted laser desorption ionization (MALDI) system (Spectroglyph Company LLC, Laurel, MD). The front panel with the MALDI translational stage was replaced with a specially developed plate with an inserted ion-transfer capillary. Pressure in the ion funnel was set at 10 Torr. Mass spectra were recorded by Orbitrap with a resolving power of 140 000. For the ionization, we used a vacuum UV lamp (Chromdet-Ecology Company, Russia). This glow discharge lamp is filled with Kr and produces photons with energies of 10 and 10.6 eV. No dopants were used. Ions were detected in a positive mode. A detailed description of the experimental setup is described elsewhere (Kostyukevich et al., 2018).

2.6. Image data acquisition

Images of grilled chickens were acquired using a DFK 33UX250 camera (The Imaging Source Europe GmbH, Bremen, Germany) placed 25 cm on the top of a grill pan. The images based on an RGB color mode were obtained and were transmitted to the computer via a USB port. We analyzed images taken for one side only not to be influenced by sample

specific features. The images from each cooking time, namely 10, 20, 30, and 40 min, were used for the analysis. Image preprocessing, image segmentation, and color measurement were performed using MATLAB® software (The MathWorks, Inc., Natick, MA). The average value in RGB was taken as the color of the sample.

2.7. Pattern recognition analysis

Linear discriminant analysis (LDA), a supervised statistical method, was applied to the data obtained from both electronic nose and computer vision; it enables classification of distinct "patterns" by reducing dimensions of multidimensional data at artificial space of features to get the maximum ratio between inter-class and in-class variations (Fedorov et al., 2017; Hierlemann & Gutierrez-Osuna, 2008). We projected the analyzed data into a coordinate system of the first two LDA components. To quantify selectivity, we evaluated Mahalanobis distance (MD), i.e. distance between clusters gravity centers in the LDA artificial space (Hierlemann & Gutierrez-Osuna, 2008).

For analysis of the contribution of each sensor, we used the Decision Tree classification method (Breiman et al., 2017; Breiman, 2001) that, following successful classification, allowed us to compute the importance of a feature as the normalized total reduction of the criterion brought by the one.

2.8. Sensory evaluation of the grilled chicken

Sensory analysis was performed to evaluate the degree of doneness, consumer appreciation, and other attributes of the grilled chicken. A panel included 16 panelists, i.e. PhD students and researchers of Laboratory of Nanomaterials, Skolkovo Institute of Science and Technology, and researchers from Alferov University. The panelists' age ranged from 24 to 48 years; the panel included 14 men and 2 women. The recruited panelists were non-smokers; they were asked to avoid using strong smells or odors for at least an hour before the evaluation, also not to use any perfume or cosmetics.

The chicken breasts were grilled according to the protocol described in Section 2.1 for 10, 20, 30, and 40 min, positioned on coded plates, and then cut into small pieces. We offered cucumber, watermelon, and water to the panelists between the samples (Ventanas et al., 2020).

The panelists assessed the following attributes: overall tenderness, tenderness liking, tenderness doneness, overall juiciness, juiciness liking, juiciness doneness, overall flavor intensity, flavor liking, flavor doneness, overall color/appearance, its liking, and doneness accordingly; also they gave an estimate of the overall liking and overall doneness (see Supplementary Materials for the example of the questionnaire). The panelist instructions were to evaluate each attribute using a 10-point hedonic scale, with 1 to be extremely tough, dry, disliked, uncooked, no flavor, or discolored and 10 meaning extremely tender, juicy, overcooked, extremely intense flavor or colored accordingly (Aaslyng, Jensen, & Karlsson, 2018; Tkacz et al., 2021; Vidal et al., 2020). Based on the assessment results, we have calculated the mean marks given by the panelists, standard deviation, and also performed normal (Gauss) distribution fitting.

3. Results and discussion

3.1. Evaluation of cooking state by e-nose

Cooking state, i.e. the quality of the final product during grilling, is determined by occurring physicochemical changes, which lead to the appearance of gas vapors, including aerosol particles; also by changes in color and texture. We detected the differences in the gaseous environment using the e-nose; typical sensor responses are shown in Fig. 1a. The response values of all the sensors demonstrate an increase in resistance, first, when the charcoal was burnt for about 20–25 min. These sensor responses can be associated primarily with CO_2, CH_4, CO, NO_x vapors emitted from burning charcoal (Estrellan & Iino, 2010; Jetter et al., 2012). The onset of grilling was also expressed in the growth in resistance of the sensors in the array, well-pronounced for the first 10 min of cooking. The measured temperature of the chicken breast surface was 190–210 °C. At such elevated temperatures, we anticipate VOCs to be formed through the Maillard reaction, thermal degradation of lipid, and Maillard–lipid interactions. Hui and Guerrero-Lagarreta reported that sulfurous compounds including 2-methyl-3-furanthiol, 2-furfurylthiol, and methionol; and carbonyl compounds such as hexanal, *trans*-2-octenal, and *trans*-2-nonenal to be the main contributors to chicken odors (Hui & Guerrero-Legarreta, 2010). Furthermore, a large number of heterocyclic compounds are produced during the chicken grilling due to high-temperature conditions (Jayasena et al., 2013). The acquired resistance values or sensors' responses we consider further as a "fingerprint" of a particular cooking state, related to the response of all the sensors to the complex mixture of VOCs formed (Lashkov et al., 2020). After grilling for 15 min, the resistance started decreasing, which should be associated with a lower amount of precursors available to form VOCs. Such a decrease is followed by a rather pronounced drop in the normalized response when the chicken begins to be overcooked.

The relative change in resistance of the e-nose sensors obtained in every cooking period is shown in Fig. 1d. There are only a few sensors characterized by a rather pronounced response to the aroma of the grilled chicken. In particular, MQ-3 and MQ-7 exhibit the highest change towards it at all the cooking times, responding mainly to alcohol vapor, and CO. MQ-2 and MQ-4 sensors also demonstrate good sensitivity to be matched to acyclic saturated hydrocarbons. Notably, the applied sensors are characterized by rather high cross-sensitivity and react to a broad range of organic compounds (Liu et al., 2012).

Thus, the e-nose provides a digital fingerprint of the volatile compounds to be recognized as a whole mixture or pattern instead of decomposition to single components (Ötles, 2016). To assign the changes of sensors resistance to an exact cooking state we have employed LDA for processing the vector signal of 8 sensors from the array (excluding humidity and temperature) as depicted in Fig. 1b. The discriminant functions component 1 and component 2 respectively represent 57.8% and 35.8% of the total variance, which indicates that they adequately explain the total variance in the dataset. It can be seen that different stages of cooking are distributed along with component 1 from the right to the left part of the plots. This explains a trend related to the changes in VOCs during cooking and separating the grilling chicken into different clusters according to the degree of readiness. First, the "under-cooked" cluster is observed within 10 min grilling time. Then, the responses related to chicken cooked for 20 and 30 min are separated in the other cluster. Further looking at the LDA plot, it can be seen that the "over-cooked" cluster is distinguished along with component 1 and component 2 after 40 min of grilling. This might be a consequence of a greater degree of tissue decomposition involving the carbonization of the chicken and corresponding processes (Coggins, 2012). The MD between the clusters is applied as a measure of the quality of selective recognition (the data are shown in Supplementary Materials, Table S1). The MD between clusters enlarges with the increase of grilling time. For instance, the MD between 10 and 40 min cooking time is 83.2, while the MD between 20 and 30 min cooking time is 19.1. The presented results indicate that e-nose could be used to distinguish the different states of chicken grilled at various cooking times. United States Department of Agriculture Food Safety and Inspection Service released approximate chicken cooking times: when breast halves, bone-in chicken is cooked by grilling, the optimum cooking time based is 10–15 min per side (USDA, 2000). Therefore, in this study, the chicken is considered to be "well-cooked" at 30 min.

While the responses of the sensors show rather pronounced differences, we analyzed each sensor contribution by performing feature importance analysis of sensors taken from the "present" condition to the previous condition, across all cooking states. When each sensor is considered as a feature, in the frame of the Decision Tree classification

method, we compared its importance coefficient (see Fig. 1c). The higher the value of the importance coefficient the greater the contribution of the feature. The values of sensors' importance at 10 min suggest that features corresponding to alcohol and ammonia are more informative to distinguish between charcoal and 10 min cooking state, while the remaining features are not. Moreover, at 30 min, features corresponding to CO, LPG, and H_2 sensors also contribute to recognition. Change in the contribution of sensors shows that after the first 10–20 min there is a transition from the half-cooked chicken to a more "grilled" one.

3.2. TGA-MS, DMA, and APPI-MS analysis of volatile compounds in grilled chicken samples

We analyzed the transformation that occurred during the grilling process to assess the composition of appearing gas vapors. Fig. 2a shows the TGA results of chicken heated to 200 °C for 40 min and corresponding *m/z* ions detected during that period. Generally, the weight changes with the increase in temperature. The TGA showed that at 60 °C, the chicken lost 5% of its weight. In addition, the highest weight loss is observed at 5 min, when the temperature has reached 170 °C resulting in a 37% weight loss in the sample. By the time the temperature is stabilized at 200 °C, the sample loses about 60% of its original weight and a small percentage of weight loss is then observed until its stabilization. This loss should stem primarily from water expelled out of meat followed by the liberation of other components including products of physicochemical processes forced by the heating; the meat has a moisture content of ca. 74% (Hughes et al., 2014).

Selected ion monitoring was also performed to detect the ion current at a certain value of *m/z* that is characteristic of the compound of interest as presented in Fig. 2b–d. The ion current at *m/z* 18 (Fig. 2c) likely attributed to the parent molecule of water shows an increase at 3 min of the experimental time. This result supports the thermal analysis measurement, showing the mass loss onset at a low temperature of ca. 60 °C. Phenyl and benzene were detected to appear after 10 min of the processing manifested by an increase of ion currents at *m/z* 77 and 78 (Fig. 2c), thus, indicating the existence of aromatic compounds that presumably contribute to the chicken odor. In addition, Fig. 2b, which identified *m/z* 32, 34, 48, and 64, reveals the presence of the main contributors to chicken odor namely sulfur-containing compounds. Alcohol and hydrocarbon compounds also influenced the formation of chicken odor. The fragments from these compounds started to appear when the temperature reaches about 170 °C corresponding to *m/z* 44, 45, 46, as presented in Fig. 2d; *m/z* 44 is also due to CO_2 liberation represented by two peaks at 7 and 10 min of the experiment.

Cooking activities generate some particles that have negative health effects (Buonanno et al., 2011). Accordingly, we further studied the aerosol particles released during cooking (Fig. 3a) as the presence of an aerosol (or fog) might affect or even disturb electronic nose or computer vision. The aerosol particle size distributions (provided by DMA) show a monomodal shape, implying the emitted species agglomerates within a single mechanism and is relatively liquid due to the characteristic lack of

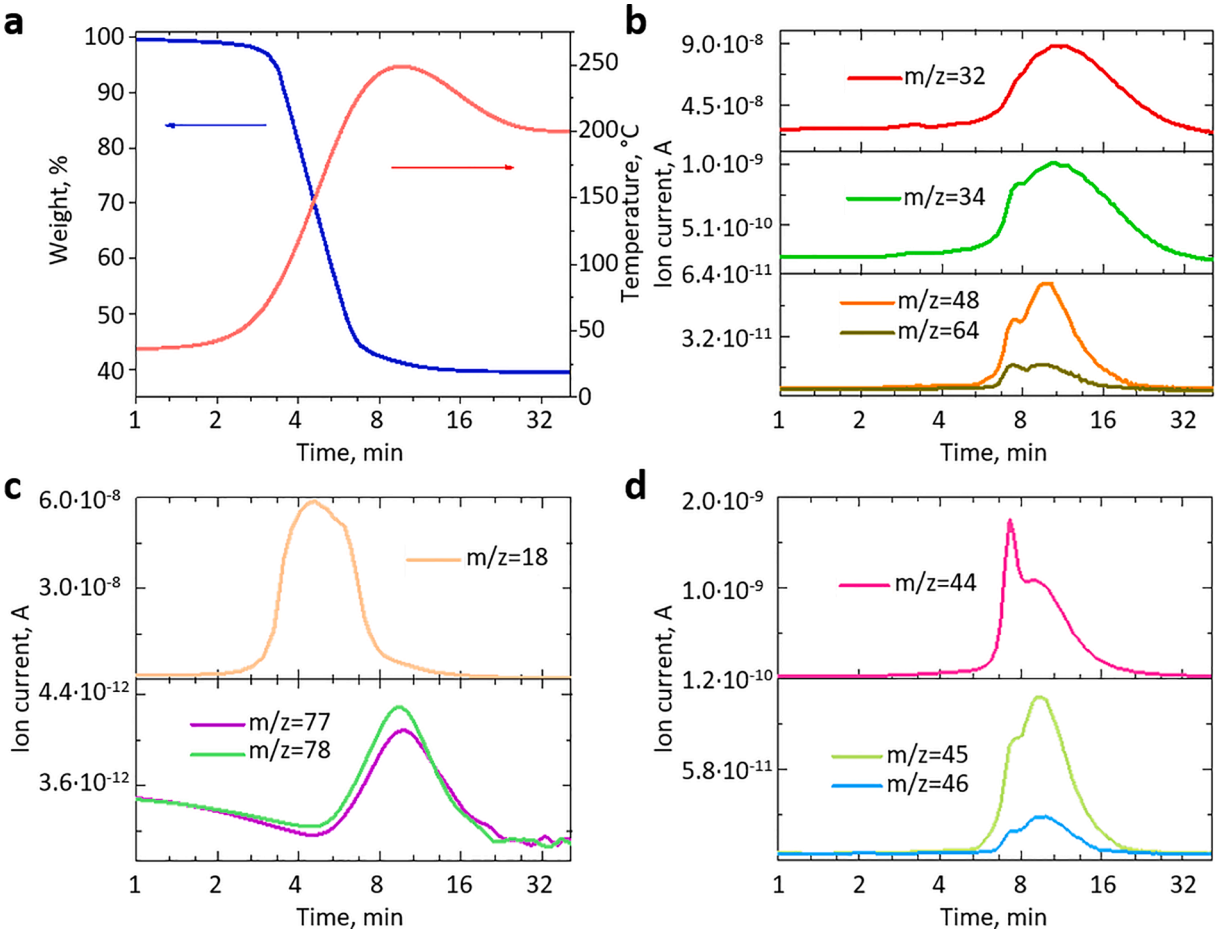

Fig. 2. Results of thermal analysis coupled with mass spectrometry. (a) The thermogravimetric curve for chicken meat heated to 200 °C in dry air with a heating rate of 50 °C/min. The blue line shows the weight changes, while the red line corresponds to the changes in temperature. (b) The fragments of sulfur-containing compounds detected in selected ion monitoring, *m/z* = 32, 34, 48, 64. (c) Selected ion monitoring of water and aromatic compounds, *m/z* = 18, 77, 78. (d) The analytes related to the molecule of alcohol, hydrocarbon, and carbon dioxide identified by mass spectrometry, *m/z* = 44, 45, 46. (For interpretation of the references to color in this figure legend, the reader is referred to the web version of this article.)

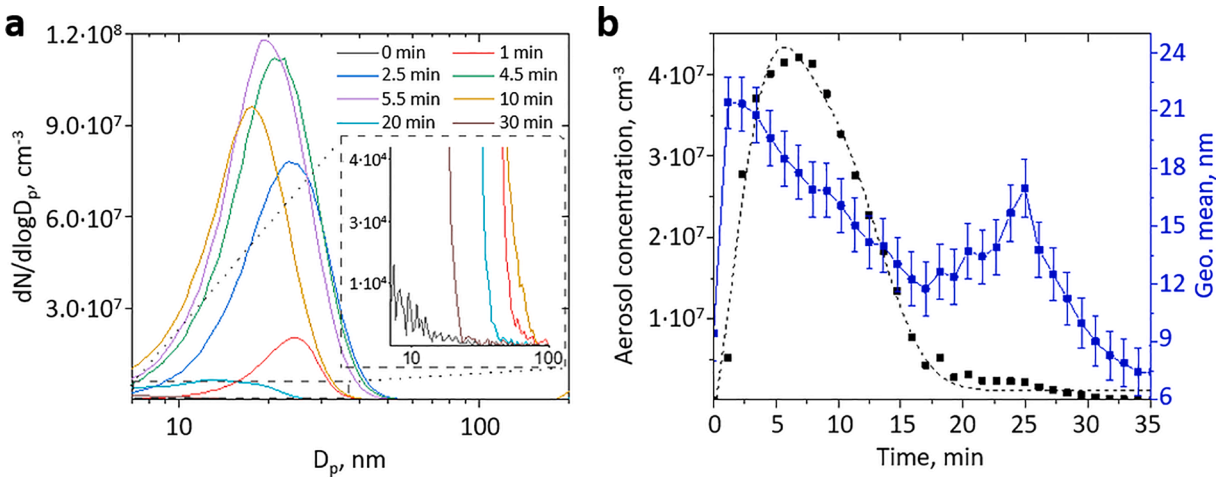

Fig. 3. Differential mobility analysis of aerosol particles emitted from the chicken at different periods of the simulated cooking process. (a) Typical particle size distributions from the experiment; the inset shows the baseline of the filtered air used for the experiment. (b) The evolution of total aerosol concentration (black dots) and geometric mean effective size (blue dots). (For interpretation of the references to color in this figure legend, the reader is referred to the web version of this article.)

the di-, tri-, and tetramers of the aerosol nanoparticles, which can be observed as specific shoulders at sizes greater than the mean one. This is the case for low-temperature agglomeration of solids, while liquid aerosol particles tend to reconstruct a spherical shape (Krasnikov et al., 2019). Grilling results in the aerosol concentration of nanoparticles reaching as high as 4.2×10^7 per cm^3 observed at 5–10 min. Taking into account the mass spectrometry results (Fig. 2), we can imply the emitted aerosol to be mainly represented by water, i.e. fog. Further decrease of the aerosol concentration can be attributed to the reduced water loss near the "optimal stage" of cooking. This DMA result is in good agreement with the thermal analysis, showing that at 5–10 min, a high percentage of the weight loss occurs, which may cause a number of compounds to be released as aerosol nanoparticles. It should be noted that the mean effective diameter, as well as aerosol concentration,

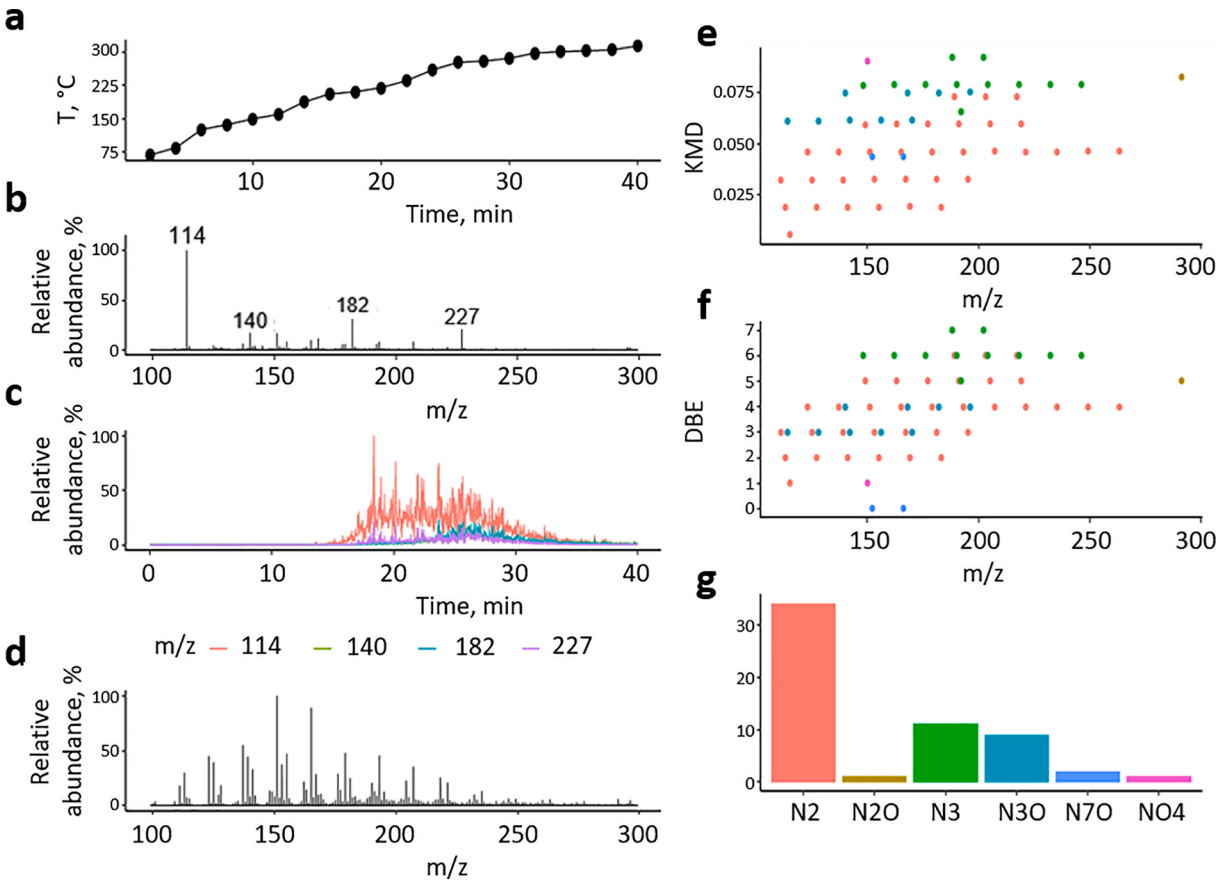

Fig. 4. Results of the mass-spectrometry experiment. (a) The heating curve. (b, c) Representative mass spectrum, and the extracted ion curves (EICs) for the most abundant peaks in the time range of 15–32 min. (d) Representative mass spectrum in the time range of 32–40 min. (e) Kendrick mass defect (KMD) plot. (f) Double-bond equivalent (DBE) plot. (g) Class distribution of detected volatile organic compounds.

slightly increases in the time range of 17–25 min (Fig. 3b). This can be also attributed to the emission of water observed as an extra shoulder in Fig. 2c. Thus, the results of aerosol studies show a massive emission of aerosol. Nevertheless, as the contribution of the humidity sensor is not the most significant one, the aerosol emission problem can be handled by a proper selection of the sensors for e-nose.

We evaluated the vapor composition during the chicken cooking process using mass spectrometry. Spectra were recorded by a built-in-house thermo-desorption system coupled with atmospheric pressure photoionization-mass spectrometry (APPI-MS) during the heating gradient as presented in Fig. 4a. According to the volatile organic compounds found in vapor, the cooking process can be divided into three time ranges with characteristic mass spectra. For the first 15 min of the heating process, we observed minor differences from the spectrum obtained without a sample. During the next time range (15–27 min), we found a few intensive peaks in mass spectrum whose intensity decreased from 27 to 35 min to background noise levels (Fig. 4b, c). In the last time range (from 35 min) spectra contained peaks from multiple compounds (Fig. 4d). The general shape of the mass spectrum and major classes of compounds resemble those previously observed for the biomass after thermal treatment (Kostyukevich et al., 2016) (Kostyukevich et al., 2017) and for biological tissues after very long exposure in a dry and hot environment (Kostyukevich et al., 2019). For the most abundant peaks (noise level was set at 5% of the highest peak) we assigned molecular formulas and plotted Kendrick mass defect (KMD, Fig. 4e), double-bond equivalent (DBE, Fig. 4f) diagram, and class distribution plot. KMD allows the detection of the compounds which are associated with the same homology series produced by $–CH_2–$ or other repeating units, whereas DBE explains the degree of unsaturation that determines π bonds and the number of rings. Unequivocal structure identification is not possible but we can see that most compounds belonging to N_2 class (Fig. 4g) started appearing at about 200 °C when severe thermal decomposition began. Our results correlate with previously published data where a large number of pyrazines were detected by GC–MS in fried chicken (Jian et al., 1983).

Cooking time and temperature affect greatly the chemical changes that occur in chicken during grilling. Our studies using TGA-MS, DMA, and APPI-MS demonstrated that chicken loses weight in the first 10 min of cooking leading to the formation of a large amount of aerosol particles. Aromatics, sulfur-containing compounds, alcohols, and hydrocarbons were presumably released during this time, resulting in the characteristic odor of cooked chicken.

3.3. Image processing analysis

Another important indicator for consumer acceptance of grilled chicken is color. In fact, the color of the chicken is influenced by chemical composition, water content, the temperature of grilling, and cooking time (Coggins, 2012). The colors represented by the mean of RGB were obtained from the grilled chicken at different cooking times (Fig. 5a). We observed that after 20–30 min of grilling, the chicken surface started to brown. Subsequently, the development of brownish darker color occurred with increase of the cooking time. The color of cooked meat is influenced by the oxidation state of iron and the complex formed by myoglobin pigment with other molecules (MacDougall, 1986). During the cooking process, iron in myoglobin is oxidized, loses its ability to bind oxygen, but forms a complex that interacts with other molecules that shifts meat color towards brown or discolored. Denaturation of myoglobin with cooking will lead to the formation of ferrohemochrome, Fe^{2+}, which is rapidly oxidized to ferrihemochrome, Fe^{3+}. The final color of cooked meat depends on the ferri/ferro ratio, which is determined by the intensity and time of cooking (Hui & Guerrero-Legarreta, 2010).

LDA was applied to the color values of chicken for the discrimination of its doneness during grilling (Fig. 5b). A score plot for the first two components explains the different samples with different cooking times.

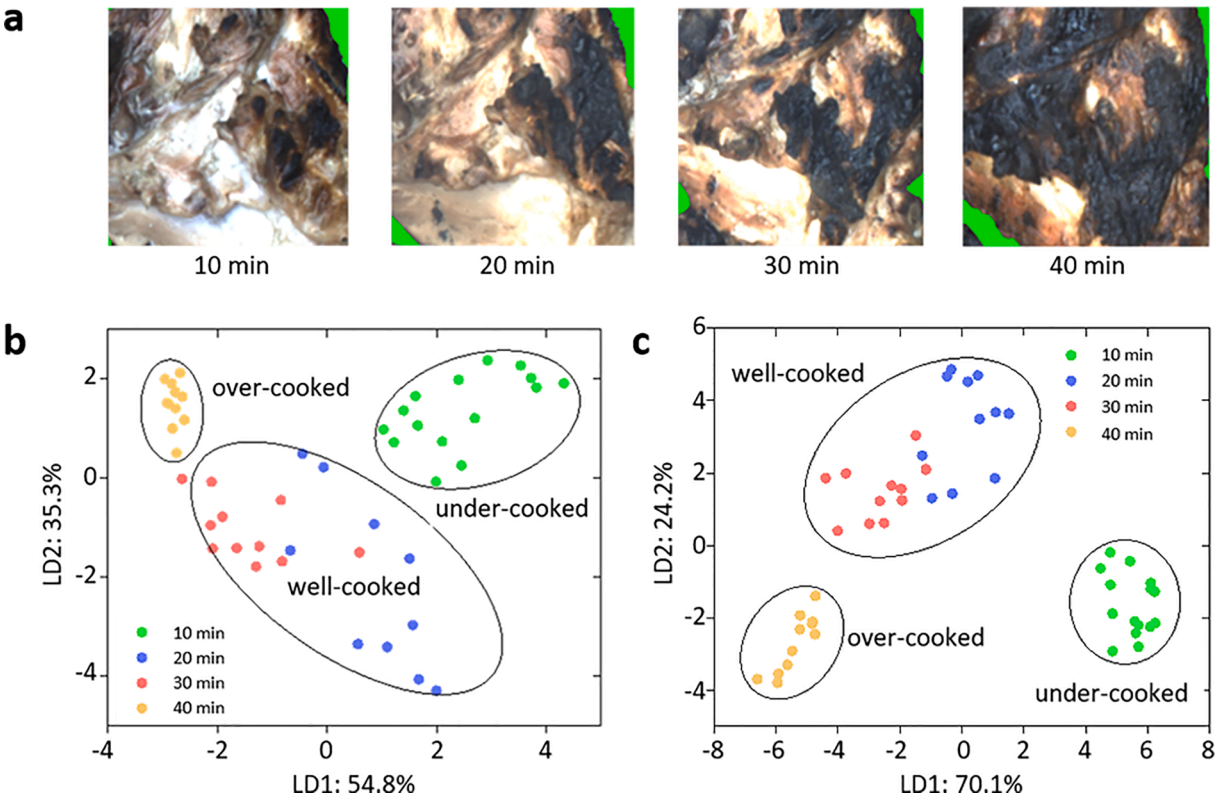

Fig. 5. Recognition of doneness degree of the grilled chicken using computer vision alone and in combination with e-nose data. (a) The images of chicken at different cooking times. (b) Recognition of doneness by LDA processing of computer vision data. (c) Recognition of doneness based on e-nose and computer vision data.

Also, LD1 explained 54.8% of the total variation, while LD2 explained 35.3% giving a sum of 90.1%. Plots of the first two discriminant functions show a reasonable separation of the samples depending on their cooking times. The MD between the "under-cooked" sample and "over-cooked" sample is 27.4. (The MD of computer vision is shown in Supplementary Materials, Table S2). Other approaches applied for the classification of computer vision results are presented in Fig. S1 (Supplementary Materials). The recognition quality might be refined even more accurately by including an assessment of each side of the chicken in computer vision protocols.

3.4. Combination of e-nose and computer vision

An advanced LDA plot could be obtained by combining the computer vision features to the responses of the e-nose. The variance of the array output falls with the square root of the number of sensors in the array (Hierlemann & Gutierrez-Osuna, 2008). Therefore, to provide a justified comparison with the e-nose, we assembled a new data set consisting of values from the five most significant gas sensors and three RGB values. Fig. 5c shows new LDA score plots for chicken grilled at different cooking times. The figure shows that the cooking stages are separated into different clusters. The MD between 10 min and 40 min cooking time is 120. It is also noticeable that the MD between the sample at 20 and 30 min of cooking time is characterized by a value of 17 (see Supplementary Materials, Table S3). Although e-nose or computer vision alone offers a good classification, combining both techniques leads to improved selectivity.

However, it is worth noting when chicken tissues with other parameters (i.e. fat content, thickness, age, etc.) or other cooking methods are considered, we anticipate different odor/color profiles that the e-nose, and computer vision should be trained for (Fedorov et al., 2017). In particular, tissue parameters (i.e. content of water, proteins, lipids) (Demby & Cunningham, 1980) would determine conductivity, specific heat capacity will influence temperature profile, together with process parameters like surrounding medium type and temperature, heat flux direction (Chen, Marks, & Murphy, 1999; Cover, 1943; Dominguez-Hernandez, Salaseviciene, & Ertbjerg, 2018; Eberth, Neal, & Robles Hernandez, 2012; van der Sman, 2012). The skin (or its absence) will also influence doneness (Pleva et al., 2020). By contact with "heat", the tissue experiences a water loss, protein denaturation, shrinkage of protein network, and the reduction of water-holding capacity (Rabeler & Feyissa, 2018) along with other physical changes (for fats) and chemical reactions of lipids (Murphy et al., 2001; Wattanachant, Benjakul, & Ledward, 2005). Accounting for that, the major variables to determine the doneness should be cooking temperature, time, and heating method (Aaslyng et al., 2003; Unklesbay et al., 1988) that all determine such characteristics as juiciness, tenderness, color, and flavor (Choi et al., 2016). At high temperatures, typical for grilling, the observed heavy water loss is expected to be negatively correlated with juiciness (Aaslyng et al., 2003) and have a great influence on its tenderness (Ježek et al., 2019).

3.5. Sensory evaluation

We further carried out sensory evaluation tests of the grilled chicken breasts to match the results obtained by analytical methods with its perception by humans (Fig. 6). As intuitively expected, during grilling the mean estimates of tenderness and juiciness are characterized by the highest values for the 10 min of cooking and then decrease almost linearly as the grilling time was increased (Fig. 6a). Conversely, the flavor intensity increases as grilling progresses showing a linear trend according to the panelist estimates. In the case of color/appearance intensity, the highest marks were given to the chicken grilled for 20 and 30 min, while for 40 min of grilling the mean marks were the lowest, possibly related to discoloration of the sample. Images of typical examples of grilled chicken breasts are shown in Supplementary Materials

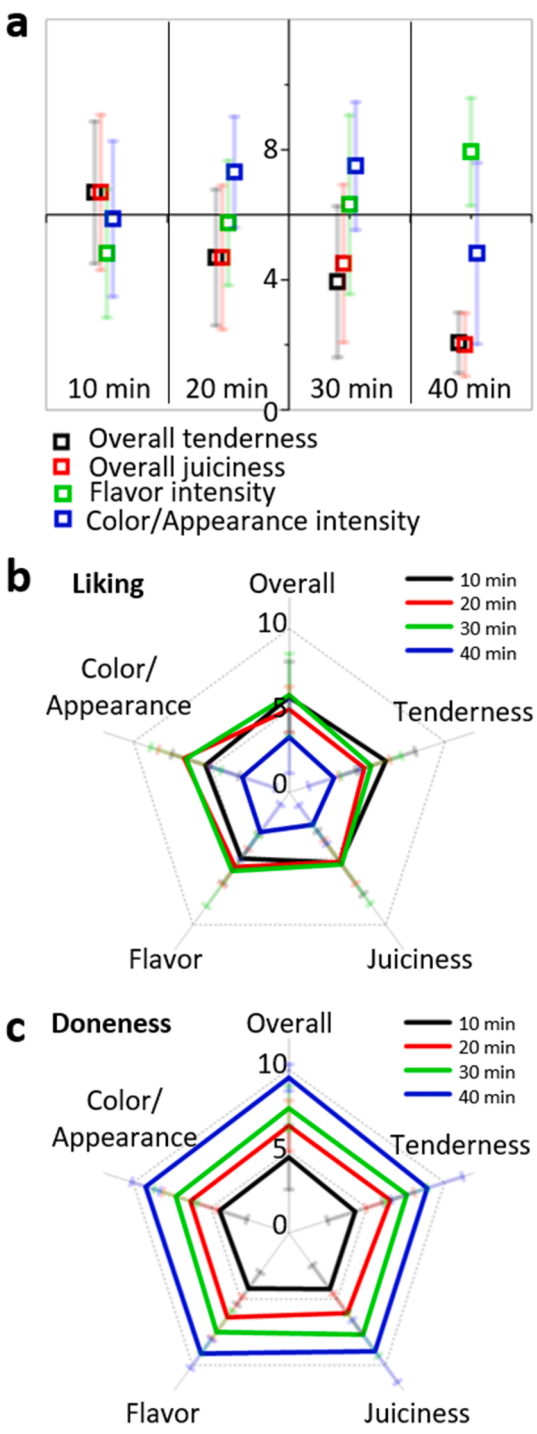

Fig. 6. Sensory evaluation of chicken breasts grilled for 10, 20, 30, and 40 min. (a) Mean marks for overall tenderness, juiciness, flavor intensity, and color/appearance with plotted standard deviations. Mean estimates for (b) liking and (c) doneness based on tenderness, juiciness, flavor, and color/appearance with standard deviations indicated.

(Fig. S3). As for the liking criteria, the mean estimates of panelists are depicted in Fig. 6b; the detailed distribution is shown in Fig. S4a. The liking of tenderness received the highest mean mark for 10 min of grilling, to be about 6.2 ± 1.9 out of 10, while the mean marks for 20 and 30 min of grilling are close to 5 out of 10. The liking of juiciness seems to be similar for 10, 20, and 30 min of grilling. Color/appearance and flavor liking are assessed to be greater at 20 and 30 min of grilling, correlating well with an increase of intensity, i.e. as depicted in Fig. 6a.

It is slightly lower for 10 min of cooking. The best mean marks of overall liking are given to the samples grilled for 30 min and 10 min, while the 40 min sample received the lowest mean marks.

The mean marks of the panelist assessment of doneness are presented in Fig. 6c. We notice a trend of an increase of mean mark with the grilling time. The samples grilled for 10 min received mean mark for all attributes to be from 4.2 to 4.6, while it was 6.0–6.6 and 7.3–7.7 for 20 and 30 min, and 9.1–9.5 for 40 min of grilling indicating overcooked chicken. The data suggest that the marks for 20 and 30 min of grilling lie closer to each other when compared to the distance between 10 and 20 min, or 30 and 40 min (the distribution is shown in Fig. S4b). Even though the marks of 10 min sample are close to the middle of the hedonic scale, we believe, that accounting for the liking (Fig. 6b) and the overall attribute marks (Fig. 6a), it might need an extra grilling time for safety reasons.

4. Conclusion

In this study, e-nose and computer vision were applied to determine the degree of doneness of a grilled chicken supported by sensory evaluation. In particular, the odor changes during the cooking process were evaluated by e-nose, while the appearance was determined by computer vision. The difference in the cooking state was obtained by applying LDA to the e-nose vector response and RGB data. The development of odor from grilled chicken was governed by water loss during cooking, releasing volatile compounds such as aromatic and sulfur-containing compounds. Moreover, we observed the presence of a high concentration of aerosol particles at 5–10 min. The appearance of chicken was also influenced by grilling time, with increase in the discoloration of chicken as time progressed. LDA resulted in good separation of clusters related to “under-cooked”, “well-cooked” and “over-cooked” chicken. A combination of e-nose and computer vision ensured greater selectivity manifested in enhanced Mahalanobis distance between clusters at the LDA plot. Thus, the proposed techniques are attractive to food quality control due to their objectivity, rapidity, and non-destructive measurement.

CRediT authorship contribution statement

Fedor S. Fedorov: Conceptualization, Data curation, Formal analysis, Funding acquisition, Investigation, Methodology, Project administration, Validation, Writing - original draft, Writing - review & editing. **Ainul Yaqin:** Data curation, Investigation, Visualization, Writing - original draft. **Dmitry V. Krasnikov:** Formal analysis, Investigation, Writing - review & editing. **Vladislav A. Kondrashov:** Investigation, Writing - review & editing. **George Ovchinnikov:** Data curation, Formal analysis, Investigation, Software, Validation, Visualization, Writing - review & editing. **Yury Kostyukevich:** Formal analysis, Validation, Visualization, Writing - review & editing. **Sergey Osipenko:** Data curation, Formal analysis, Investigation, Writing - review & editing. **Albert G. Nasibulin:** Conceptualization, Formal analysis, Funding acquisition, Methodology, Project administration, Resources, Supervision, Validation, Writing - original draft, Writing - review & editing.

Declaration of Competing Interest

The authors declare that they have no known competing financial interests or personal relationships that could have appeared to influence the work reported in this paper.

Acknowledgments

F.S.F. acknowledges the Russian Science Foundation for support of STA-MS, DMA, gas sensor performance, computer vision, and a sensory evaluation by grant no. 19-72-00136. This work is supported by the Ministry of Science and Higher Education of the Russian Federation (project no. FZSR-2020-0007 in the framework of the state assignment no. 075-03-2020-097/1).

Appendix A. Supplementary data

Supplementary data to this article can be found online at https://doi.org/10.1016/j.foodchem.2020.128747.

References

Aaslyng, M. D., Jensen, H., & Karlsson, A. H. (2018). The gender background of texture attributes of pork loin. *Meat Science, 136*, 79–84. https://doi.org/10.1016/j.meatsci.2017.10.018.

Aaslyng, M. D., Bejerholm, C., Ertbjerg, P., Bertram, H. C., & Andersen, H. J. (2003). Cooking loss and juiciness of pork in relation to raw meat quality and cooking procedure. *Food Quality and Preference, 14*(4), 277–288. https://doi.org/10.1016/S0950-3293(02)00086-1.

Breiman, L., Friedman, J. H., Olshen, R. A., & Stone, C. J. (2017). Classification and regression trees. Classification and regression trees. https://doi.org/10.1201/9781315139470.

Breiman, L. (2001). Random forests. *Machine Learning, 45*(1), 5–32. https://doi.org/10.1023/A:1010933404324.

Brosnan, T., & Sun, D.-W. (2004). Improving quality inspection of food products by computer vision—A review. *Journal of Food Engineering, 61*(1), 3–16. https://doi.org/10.1016/S0260-8774(03)00183-3.

Buonanno, G., Johnson, G., Morawska, L., & Stabile, L. (2011). Volatility characterization of cooking-generated aerosol particles. *Aerosol Science and Technology, 45*(9), 1069–1077. https://doi.org/10.1080/02786826.2011.580797.

Chen, H., Marks, B. P., & Murphy, R. Y. (1999). Modeling coupled heat and mass transfer for convection cooking of chicken patties. *Journal of Food Engineering, 42*(3), 139–146. https://doi.org/10.1016/S0260-8774(99)00111-9.

Chen, L.-Y., Wu, C.-C., Chou, T.-I., Chiu, S.-W., & Tang, K.-T. (2018). Development of a dual MOS electronic nose/camera system for improving fruit ripeness classification. *Sensors, 18*, 3256. https://doi.org/10.3390/s18103256.

Choi, Y.-S., Hwang, K.-E., Jeong, T.-J., Kim, Y.-B., Jeon, K.-H., Kim, E.-M., … Kim, C.-J. (2016). Comparative study on the effects of boiling, steaming, grilling, microwaving and superheated steaming on quality characteristics of marinated chicken steak. *Food Science of Animal Resources (한국축산식품학회지), 36*(1), 1–7. https://doi.org/10.5851/kosfa.2016.36.1.1.

Chung, S., Yettella, R., Kim, J., Kwon, K., Kim, M., & Min, D. (2011). Effects of grilling and roasting on the levels of polycyclic aromatic hydrocarbons in beef and pork. *Food Chemistry, 129*, 1420–1426. https://doi.org/10.1016/j.foodchem.2011.05.092.

Coggins, P. C. (2012). Attributes of muscle foods: Color, texture, flavor. In Handbook of meat, poultry and seafood quality (pp. 35–44). John Wiley & Sons, Ltd. https://doi.org/10.1002/9781118352434.ch3.

Cover, S. (1943). Effect of extremely low rates of heat penetration on tendering of beef. *Journal of Food Science, 8*(5), 388–394. https://doi.org/10.1111/j.1365-2621.1943.tb16573.x.

Da Costa, N. C., & Eri, S. (2012). Chemical characterization. In Handbook of meat, poultry and seafood quality (pp. 76–90). John Wiley & Sons, Ltd. https://doi.org/10.1002/9781118352434.ch6.

Demby, J. H., & Cunningham, F. E. (1980). Factors affecting composition of chicken meat. A literature review. *World's Poultry Science Journal, 36*(1), 25–67. https://doi.org/10.1079/WPS19800002.

Di Rosa, A. R., Leone, F., Cheli, F., & Chiofalo, V. (2017). Fusion of electronic nose, electronic tongue and computer vision for animal source food authentication and quality assessment – A review. *Journal of Food Engineering, 210*, 62–75. https://doi.org/10.1016/j.jfoodeng.2017.04.024.

Dolara, P., Commoner, B., & Vithayathil, A. (1979). The effect of temperature on the formation of mutagens. *Cooking Procedures, 60*, 231–237.

Dominguez-Hernandez, E., Salaseviciene, A., & Ertbjerg, P. (2018). Low-temperature long-time cooking of meat: Eating quality and underlying mechanisms. *Meat Science, 143*, 104–113. https://doi.org/10.1016/j.meatsci.2018.04.032.

Dong, W., Hu, R., Long, Y., Li, H., Zhang, Y., Zhu, K., & Chu, Z. (2019). Comparative evaluation of the volatile profiles and taste properties of roasted coffee beans as affected by drying method and detected by electronic nose, electronic tongue, and HS-SPME-GC-MS. *Food Chemistry, 272*, 723–731. https://doi.org/10.1016/j.foodchem.2018.08.068.

Du, C.-J., & Sun, D.-W. (2006). Learning techniques used in computer vision for food quality evaluation: A review. *Journal of Food Engineering, 72*(1), 39–55. https://doi.org/10.1016/j.jfoodeng.2004.11.017.

Eberth, J. F., Neal, J. A., & Robles Hernandez, F. C. (2012). Evaluation of heat propagation through poultry in a reduced computational-cost model of contact cooking. *International Journal of Food Science & Technology, 47*(6), 1130–1137. https://doi.org/10.1111/j.1365-2621.2012.02951.x.

Estrellan, C., & Iino, F. (2010). Toxic emissions from open burning. *Chemosphere, 80*, 193–207. https://doi.org/10.1016/j.chemosphere.2010.03.057.

FAO. (2018). *World food and agriculture statistical pocketbook 2018*. Food and Agriculture Organization of The United Nations.

Farroni, A., & del Pilar Buera, M. (2012). Colour and surface fluorescence development and their relationship with maillard reaction markers as influenced by structural changes during cornflakes production. *Food Chemistry, 135*(3), 1685–1691. https://doi.org/10.1016/j.foodchem.2012.05.114.

Fedorov, F., Podgainov, D., Varezhnikov, A., Lashkov, A., Gorshenkov, M., Burmistrov, I., … Sysoev, V. (2017). The potentiodynamic bottom-up growth of the tin oxide nanostructured layer for gas-analytical multisensor array chips. *Sensors, 17*(8), 1908. https://doi.org/10.3390/s17081908.

Fedorov, F., Vasilkov, M., Lashkov, A., Varezhnikov, A., Fuchs, D., Kübel, C., … Sysoev, V. (2017). Toward new gas-analytical multisensor chips based on titanium oxide nanotube array. *Scientific Reports, 7*(1), 9732. https://doi.org/10.1038/s41598-017-10495-8.

Girolami, A., Napolitano, F., Faraone, D., Di Bello, G., & Braghieri, A. (2014). Image analysis with the computer vision system and the consumer test in evaluating the appearance of lucanian dry sausage. *Meat Science, 96*(1), 610–616. https://doi.org/10.1016/j.meatsci.2013.08.006.

Gökmen, V., Şenyuva, H. Z., Dülek, B., & Çetin, A. E. (2007). Computer vision-based image analysis for the estimation of acrylamide concentrations of potato chips and French fries. *Food Chemistry, 101*(2), 791–798. https://doi.org/10.1016/j.foodchem.2006.02.034.

Greiff, K., Mathiassen, J. R., Misimi, E., Hersleth, M., & Aursand, I. G. (2015). Gradual reduction in sodium content in cooked ham, with corresponding change in sensorial properties measured by sensory evaluation and a multimodal machine vision system. *PLOS ONE, 10*(9), 1–14. https://doi.org/10.1371/journal.pone.0137805.

Gunasekaran, S. (1996). Computer vision technology for food quality assurance. *Trends in Food Science & Technology, 7*(8), 245–256. https://doi.org/10.1016/0924-2244(96)10028-5.

Hassan, G. M., Magda, R. A., & Awad, A. A. (2010). Nutritional, biochemical and cytogenotoxicity studies on wasted fat released from chicken during grilling process. *Food and Chemical Toxicology, 48*(10), 2675–2681. https://doi.org/10.1016/j.fct.2010.06.039.

Hierlemann, A., & Gutierrez-Osuna, R. (2008). Higher-order chemical sensing. *Chemical Reviews, 108*(2), 563–613. https://doi.org/10.1021/cr068116m.

Hines, E. L., Boilot, P., Gardner, J. W., & Gongora, M. A. (2002). Pattern analysis for electronic noses. *Handbook of Machine Olfaction*. https://doi.org/10.1002/3527601597.ch6.

Hirano, S. H., Brubaker, J. R., Patterson, D. J., & Hayes, G. R. (2013). Detecting cooking state with gas sensors during dry cooking. In *UbiComp 2013 - Proceedings of the 2013 ACM International Joint Conference on Pervasive and Ubiquitous Computing* (pp. 411–414). https://doi.org/10.1145/2493432.2493523.

Huang, L., Zhao, J., Chen, Q., & Zhang, Y. (2014). Nondestructive measurement of total volatile basic nitrogen (TVB-N) in pork meat by integrating near infrared spectroscopy, computer vision and electronic nose techniques. *Food Chemistry, 145*, 228–236. https://doi.org/10.1016/j.foodchem.2013.06.073.

Hughes, J. M., Oiseth, S. K., Purslow, P. P., & Warner, R. D. (2014). A structural approach to understanding the interactions between colour, water-holding capacity and tenderness. *Meat Science, 98*(3), 520–532. https://doi.org/10.1016/j.meatsci.2014.05.022.

Hui, Y. H., & Guerrero-Legarreta, I. (2010). Sanitation requirements. In Handbook of poultry science and technology: Volume 2 (Vol. 2, pp. 545–572). https://doi.org/10.1002/9780470504475.ch37.

Iakovlev, V. Y., Krasnikov, D. V., Khabushev, E. M., Kolodiazhnaia, J. V., & Nasibulin, A. G. (2019). Artificial neural network for predictive synthesis of single-walled carbon nanotubes by aerosol CVD method. *Carbon, 153*, 100–103. https://doi.org/10.1016/j.carbon.2019.07.013.

Jackman, P., & Sun, D.-W. (2013). Recent advances in image processing using image texture features for food quality assessment. *Trends in Food Science & Technology, 29*(1), 35–43. https://doi.org/10.1016/j.tifs.2012.08.008.

Jayasena, D. D., Ahn, D. U., Nam, K. C., & Jo, C. (2013). Flavour chemistry of chicken meat: A review. *Asian-Australasian Journal of Animal Sciences, 26*(5), 732–742. https://doi.org/10.5713/ajas.2012.12619.

Jetter, J., Zhao, Y., Smith, K. R., Khan, B., Yelverton, T., DeCarlo, P., & Hays, M. D. (2012). Pollutant emissions and energy efficiency under controlled conditions for household biomass cookstoves and implications for metrics useful in setting international test standards. *Environmental Science & Technology, 46*(19), 10827–10834. https://doi.org/10.1021/es301693f.

Ježek, F., Kameník, J., Macharáčková, B., Bogdanovičová, K., & Bednář, J. (2019). Cooking of meat: Effect on texture, cooking loss and microbiological quality – A review. *Acta Veterinaria Brno, 88*(4), 487–496. https://doi.org/10.2754/avb201988040487.

Jian, T., Jin, Q. Z., Shen, G.-H., Ho, C.-T., & Chang, S. S. (1983). Isolation and identification of volatile compounds from fried chicken. *Journal of Agricultural and Food Chemistry, 31*(6), 1287–1292. https://doi.org/10.1021/jf00120a035.

Jordan, M. I., & Mitchell, T. M. (2015). Machine learning: Trends, perspectives, and prospects. *Science, 349*(6245), 255–260. https://doi.org/10.1126/science.aaa8415.

Joutou, T., & Yanai, K. (2009). A food image recognition system with multiple kernel learning. In *2009 16th IEEE International Conference on Image Processing (ICIP)* (pp. 285–288). https://doi.org/10.1109/ICIP.2009.5413400.

Keller, A., Gerkin, R. C., Guan, Y., Dhurandhar, A., Turu, G., Szalai, B., … Meyer, P. (2017). Predicting human olfactory perception from chemical features of odor molecules. *Science, 355*(6327), 820–826. https://doi.org/10.1126/science.aal2014.

Khabushev, E. M., Krasnikov, D. V., Zaremba, O. T., Tsapenko, A. P., Goldt, A. E., & Nasibulin, A. G. (2019). Machine learning for tailoring optoelectronic properties of single-walled carbon nanotube films. *The Journal of Physical Chemistry Letters, 10*(21), 6962–6966. https://doi.org/10.1021/acs.jpclett.9b02777.

Kostyukevich, Y., Kitova, A., Zherebker, A., Rukh, S., & Nikolaev, E. (2019). Investigation of the archeological remains using ultrahigh resolution mass spectrometry. *European Journal of Mass Spectrometry, 25*(4), 391–396. https://doi.org/10.1177/1469066719840287.

Kostyukevich, Y., Vlaskin, M., Vladimirov, G., Zherebker, A., Kononikhin, A., Popov, I., & Nikolaev, E. (2017). The investigation of the bio-oil produced by hydrothermal liquefaction of spirulina platensis using ultrahigh resolution Fourier transform ion cyclotron resonance mass spectrometry. *European Journal of Mass Spectrometry, 23*(2), 83–88. https://doi.org/10.1177/1469066717702648.

Kostyukevich, Y., Zherebker, A., Kononikhin, A., Popov, I., Perminova, I., & Nikolaev, E. (2016). The investigation of the birch tar using ultrahigh resolution Fourier transform ion cyclotron resonance mass spectrometry and hydrogen/deuterium exchange approach. *International Journal of Mass Spectrometry, 404*, 29–34. https://doi.org/10.1016/j.ijms.2016.03.012.

Kostyukevich, Y., Zherebker, A., Vlaskin, M. S., Borisova, L., & Nikolaev, E. (2018). Microprobe for the thermal analysis of crude oil coupled to photoionization Fourier transform mass spectrometry. *Analytical Chemistry, 90*(15), 8756–8763. https://doi.org/10.1021/acs.analchem.8b02043.

Krasnikov, D. V., Zabelich, B. Y., Iakovlev, V. Y., Tsapenko, A. P., Romanov, S. A., Alekseeva, A. A., … Nasibulin, A. G. (2019). A spark discharge generator for scalable aerosol CVD synthesis of single-walled carbon nanotubes with tailored characteristics. *Chemical Engineering Journal, 372*, 462–470. https://doi.org/10.1016/j.cej.2019.04.173.

Lan, C. M., Kao, T. H., & Chen, B. H. (2004). Effects of heating time and antioxidants on the formation of heterocyclic amines in marinated foods. *Journal of Chromatography B, 802*, 27–37. https://doi.org/10.1016/j.jchromb.2003.09.025.

Langsrud, S., Sørheim, O., Skuland, S. E., Almli, V. L., Jensen, M. R., Grøvlen, M. S., … Møretrø, T. (2020). Cooking chicken at home: Common or recommended approaches to judge doneness may not assure sufficient inactivation of pathogens. *PLOS ONE, 15*(4), 1–27. https://doi.org/10.1371/journal.pone.0230928.

Lashkov, A. V., Fedorov, F. S., Vasilkov, M. Y., Kochetkov, A. V., Belyaev, I. V., Plugin, I. A., … Sysoev, V. V. (2020). The Ti wire functionalized with inherent TiO2 nanotubes by anodization as one-electrode gas sensor: A proof-of-concept study. *Sensors and Actuators B: Chemical, 306*, 127615. https://doi.org/10.1016/j.snb.2019.127615.

Lee, J.-G., Kim, S.-Y., Moon, J.-S., Kim, S.-H., Kang, D.-H., & Yoon, H.-J. (2016). Effects of grilling procedures on levels of polycyclic aromatic hydrocarbons in grilled meats. *Food Chemistry, 199*, 632–638. https://doi.org/10.1016/j.foodchem.2015.12.017.

Leiva-Valenzuela, G. A., Mariotti, M., Mondragón, G., & Pedreschi, F. (2018). Statistical pattern recognition classification with computer vision images for assessing the furan content of fried dough pieces. *Food Chemistry, 239*, 718–725. https://doi.org/10.1016/j.foodchem.2017.06.095.

Lerma, N., Bellincontro, A., Mencarelli, F., Moreno, J., & Peinado, R. (2011). Use of electronic nose, validated by GC-MS, to establish the optimum off-vine dehydration time of wine grapes. *Food Chemistry, 130*, 447–452. https://doi.org/10.1016/j.foodchem.2011.07.058.

Li, C., Heinemann, P., & Sherry, R. (2007). Neural network and Bayesian network fusion models to fuse electronic nose and surface acoustic wave sensor data for apple defect detection. *Sensors and Actuators B: Chemical, 125*, 301–310. https://doi.org/10.1016/j.snb.2007.02.027.

Li, Z., Wang, S., & Xin, H. (2018). Toward artificial intelligence in catalysis. *Nature Catalysis, 1*(9), 641–642. https://doi.org/10.1038/s41929-018-0150-1.

Liu, X., Cheng, S., Liu, H., Hu, S., Zhang, D., & Ning, H. (2012). A survey on gas sensing technology. *Sensors, 12*, 9635–9665. https://doi.org/10.3390/s120709635.

MacDougall, D. B. (1986). The chemistry of colour and appearance. *Food Chemistry, 21*(4), 283–299. https://doi.org/10.1016/0308-8146(86)90063-4.

Martinez, A. M., & Kak, A. C. (2001). PCA versus LDA. *IEEE Transactions on Pattern Analysis and Machine Intelligence, 23*(2), 228–233. https://doi.org/10.1109/34.908974.

Mottram, D. S. (1998). Flavour formation in meat and meat products: A review. *Food Chemistry, 62*(4), 415–424. https://doi.org/10.1016/S0308-8146(98)00076-4.

Murphy, R. Y., Johnson, E. R., Duncan, L. K., Clausen, E. C., Davis, M. D., & March, J. A. (2001). Heat transfer properties, moisture loss, product yield, and soluble proteins in chicken breast patties during air convection cooking. *Poultry Science, 80*(4), 508–514. https://doi.org/10.1093/ps/80.4.508.

Nashat, S., & Abdullah, M. Z. (2010). Multi-class colour inspection of baked foods featuring support vector machine and Wilk's λ analysis. *Journal of Food Engineering, 101*(4), 370–380. https://doi.org/10.1016/j.jfoodeng.2010.07.022.

Ötles, S. (2016). Handbook of food analysis instruments. *Handbook of Food Analysis Instruments*.

Persaud, K., & Dodd, G. (1982). Analysis of discrimination mechanisms in the Mammalian olfactory system using a model nose. *Nature, 299*(5881), 352–355. https://doi.org/10.1038/299352a0.

Pleva, D., Lányi, K., Darnay, L., & Laczay, P. (2020). Predictive correlation between apparent sensory properties and the formation of heterocyclic amines in chicken breast as a function of grilling temperature and time. *Foods, 9*(4). https://doi.org/10.3390/foods9040412.

Ponzoni, A., Depari, A., Falasconi, M., Comini, E., Flammini, A., Marioli, D., … Sberveglieri, G. (2008). Bread baking aromas detection by low-cost electronic nose. *Sensors and Actuators, B: Chemical, 130*(1), 100–104. https://doi.org/10.1016/j.snb.2007.07.099.

Potyrailo, R. A. (2016). Multivariable sensors for ubiquitous monitoring of gases in the era of internet of things and industrial internet. *Chemical Reviews, 116*(19), 11877–11923. https://doi.org/10.1021/acs.chemrev.6b00187.

Rabeler, F., & Feyissa, A. H. (2018). Modelling the transport phenomena and texture changes of chicken breast meat during the roasting in a convective oven. *Journal of Food Engineering, 237*, 60–68. https://doi.org/10.1016/j.jfoodeng.2018.05.021.

Schroeder, V., Evans, E., Wu, Y.-C., Voll, C.-C., McDonald, B., Savagatrup, S., & Swager, T. (2019). Chemiresistive sensor array and machine learning classification

of food. *ACS Sensors, 4*(8), 2101–2108. https://doi.org/10.1021/acssensors.9b00825.

Shi, H., & Ho, C.-T. (1994). The flavour of poultry meat. In F. Shahidi (Ed.), Flavor of meat and meat products (pp. 52–70). Boston, MA: Springer US. https://doi.org/10.1007/978-1-4615-2177-8_4.

Taheri-Garavand, A., Fatahi, S., Omid, M., & Makino, Y. (2019). Meat quality evaluation based on computer vision technique: A review. *Meat Science, 156*, 183–195. https://doi.org/10.1016/j.meatsci.2019.06.002.

Tkacz, K., Wojdyło, A., Turkiewicz, I. P., & Nowicka, P. (2021). Anti-diabetic, anti-cholinesterase, and antioxidant potential, chemical composition and sensory evaluation of novel sea buckthorn-based smoothies. *Food Chemistry, 338*, 128105. https://doi.org/10.1016/j.foodchem.2020.128105.

Unklesbay, K., Keller, J., Unklesbay, N., & Subhangkasen, D. (1988). Determination of doneness of beef steaks using fuzzy pattern recognition. *Journal of Food Engineering, 8* (2), 79–90. https://doi.org/10.1016/0260-8774(88)90056-8.

USDA. (2000). Chicken from farm to table. United States Department of Agriculture - USDA, 1–8.

van der Sman, R. G. M. (2012). Thermodynamics of meat proteins. *Food Hydrocolloids, 27* (2), 529–535. https://doi.org/10.1016/j.foodhyd.2011.08.016.

Ventanas, S., González-Mohino, A., Estévez, M., & Carvalho, L. (2020). Chapter 21 - Innovation in sensory assessment of meat and meat products. In A. K. Biswas, & P. K. Mandal (Eds.), *Meat quality analysis* (pp. 393–418). Academic Press. https://doi.org/10.1016/B978-0-12-819233-7.00021-5.

Vidal, N. P., Manful, C., Pham, T. H., Wheeler, E., Stewart, P., Keough, D., & Thomas, R. (2020). Novel unfiltered beer-based marinades to improve the nutritional quality, safety, and sensory perception of grilled ruminant meats. *Food Chemistry, 302*, 125326. https://doi.org/10.1016/j.foodchem.2019.125326.

Wan, J., Jiang, J.-W., & Park, H. S. (2020). Machine learning-based design of porous graphene with low thermal conductivity. *Carbon, 157*, 262–269. https://doi.org/10.1016/j.carbon.2019.10.037.

Wang, H.-H., & Sun, D.-W. (2002). Melting characteristics of cheese: Analysis of effects of cooking conditions using computer vision technology. *Journal of Food Engineering, 51* (4), 305–310. https://doi.org/10.1016/S0260-8774(01)00072-3.

Wattanachant, S., Benjakul, S., & Ledward, D. A. (2005). Microstructure and thermal characteristics of Thai indigenous and broiler chicken muscles. *Poultry Science, 84* (2), 328–336. https://doi.org/10.1093/ps/84.2.328.

Yeh, J. C. H., Hamey, L. G. C., Westcott, T., & Sung, S. K. Y. (1995). Colour bake inspection system using hybrid artificial neural networks. In Proceedings of ICNN'95 - International Conference on Neural Networks (Vol. 1, pp. 37–42). https://doi.org/10.1109/ICNN.1995.487873.